Sensing wall-pressure fluctuations by particle image velocimetry

Fulvio Scarano, Sina Ghaemi

ACOUSTICS 2012

Sensing wall-pressure fluctuations by particle image velocimetry

F. Scarano and S. Ghaemi

TU Delft, Aerospace Engineering Dept., Kluyverweg 1, 2629HS Delft, Netherlands
f.scarano@tudelft.nl

A novel approach is introduced to measure spatio-temporal pressure fluctuations generated by airflow over the surface of solid objects. This experimental method is based on a three-dimensional time-resolved variant of particle image velocimetry technique (Tomographic-PIV). The working principle invokes the Navier-Stokes equations and is based on the evaluation of the instantaneous pressure gradient from the measurement of fluid parcels acceleration, in the assumption of incompressible flow. The experiments presented here are conducted at 10 kHz and demonstrate the applicability of the PIV-based pressure imaging to broadband pressure fluctuations from a fully developed turbulent boundary layer at outer velocity of 10 m/s, under zero-pressure gradient. The simultaneous visualization of surface pressure and velocity vector field enables to understand the dynamics of large-scale coherent flow events and their role in the generation of pressure fluctuations and sound production.

1 Introduction

The unsteady pressure field caused by turbulent airflow interacting with a solid surface is the source of several engineering problems, mostly for flow induced vibrations and aeroacoustic noise generation. The particular case of a turbulent boundary layer is relevant for cabin noise, structural vibration in aircraft and high-speed trains, and hydroacoustic emissions of submarines (Willmarth 1975). The pressure fluctuations travelling over wing edges are the source of trailing edge noise (Ffowcs Williams & Hall 1970).

From the early measurements of pressure fluctuations in a turbulent boundary layer by Willmarth (1956) it became clear that the large sensor area needed to be sensitive to the minute pressure fluctuations introduced significant attenuation of the high-frequency fluctuations, which was solved by placing the pressure transducer behind a pinhole orifice (Blake 1970). This approach was adopted during the last decades, requiring both amplitude and phase calibration of the sensor due to the resonant-frequency of the cavity (Tsuji 2007).

The investigation of the physical aspects of boundary layer pressure fluctuations were mostly conducted using conjectures based on wall-pressure measurement or Direct Numerical Simulation (DNS) databases. Johansson et al. (1987) investigated the relation between high amplitude wall pressure fluctuations and flow coherent structures using wall pressure measurement together with hot-wire measurement across the flow. Chang et al. (1999) studied the contribution of different regions of turbulent boundary layer to the spectrum of surface pressure based on a DNS data. Although DNS provides access to 3D pressure and velocity field, its extension to high Re and more complex geometries remains unpractical.

The investigation of passive and active methods for surface pressure control is also highly motivated by the industry for acoustic noise emission reduction from aerodynamic surfaces. These applications require the development of 2D or 3D non-intrusive pressure measurement techniques with appropriate spatio-temporal measurement capabilities.

The evaluation of the flow field pressure from the application of the Navier-Stokes equations to the measured velocity field by PIV has already been considered in past studies. This method offers the advantage of a simultaneous inspection of the velocity and of the pressure fluctuations. Moreover this is the only way to experimentally investigate the pressure field at the surface and in the flow and can be applied in the low speed as well as high speed regime.

Moreover the non-intrusive measurement of the pressure field is interesting in those cases where transducers cannot be installed below the surface, for instance on thin surfaces like on propeller blades and at the trailing edge. Baur and Köngeter (1999) estimated the unsteady pressure field generated by a wall-mounted obstacle and spatially integrated the unsteady Navier-Stokes equation. Liu and Katz (2006) performed two-components PIV measurements with four exposures and evaluated the material derivative of the velocity around a rectangular cavity. They showed that a 2D Lagrangian method yields an accurate estimate of the material derivative and also improved the spatial marching method of Baur and Kongeter by an omni-directional integration approach. Violato et al. (2011) extended the calculation of the material derivative to 3D particle trajectory and evaluated the pressure field of a rod-airfoil flow from time-resolved Tomo-PIV measurement. Charonko et al. (2010) assessed the effect of different approaches such as integration method, grid resolution, sampling rate and emphasized that an optimum approach highly depends on the flow type. De Kat and van Oudheusden (2011) made a theoretical and experimental study to characterize the attainable measurement precision using Stereoscopic PIV and Tomo-PIV.

As this brief summary demonstrates, the application of PIV-based pressure evaluation to turbulent boundary layers remains unexplored, which is mostly due to the three-dimensional complexity of the turbulent flow fluctuations along with the broad frequency spectrum of the wall-pressure fluctuations.

The challenge of the pressure estimation from PIV measurement in a turbulent flow rises from the wide range of length scales and the relative importance of the small-scale high-frequency structures especially in the near wall region. Instead, previous works concentrated on two-dimensional fluctuations arising from large vortical structures resulting from periodical or quasi-periodical vortex shedding at low frequency. For instance, Koschatzky et al. (2011) studied the flow in a rectangular cavity with rms pressure fluctuations of about 20 Pa and a dominant tonal frequency of 454 Hz. The pressure field within the wake of the square cylinder investigated by de Kat and van Oudheusden (2010, 2011) was conducted at a freestream velocity of 4.7 m/s with 10 Pa rms pressure fluctuation and a dominant shedding frequency of 20 Hz at the side of the cylinder while 5 Pa rms pressure fluctuation and a dominant frequency of 40 Hz at the cylinder base.

A turbulent boundary layer is a more extreme situation with small three-dimensional velocity fluctuations. The rms pressure fluctuations are as low as 1% of the free stream dynamic pressure (less than 1 Pa rms pressure fluctuations at free stream velocity of 10 m/s), with no dominant component in the energy spectral density (Tsuji et al. 2007). The structures of the inner layer are as small as 20 wall units ($\lambda+$) and have a temporal frequency of a few kHz (Farabee and Casarella 1991). This wide range of scales requires a measurement system of high spatial and temporal dynamic range to capture both the small structures within

the inner layer and also the large-scale events occurring in the outer layer.

The present study illustrates the effort undertaken to obtain the unsteady pressure field within a turbulent boundary layer from time-resolved 3D velocity fields measured by Tomo-PIV in the thin-volume configuration (Violato et al., 2011). Emphasis is placed on the characterization of the measurement accuracy of surface pressure as obtained from the PIV with integration of the Poisson equation and compared with surface pressure fluctuations measured by the condenser microphones. The effect of different parameters is evaluated such as the use of two-dimensional or three-dimensional data, the role of the numerical procedures for the evaluation of the material derivative, specifically comparing the Eulerian and Lagrangian schemes. Last but not least, the discussion covers the effect of boundary conditions on the reliability of the results.

2 Pressure from PIV

The evaluation of the instantaneous pressure field form the instantaneous 3D velocity field is based on the use of the Navier-Stokes equation. Assuming incompressible flow and constant viscosity the momentum equation reads as:

$$\nabla P = -\rho \frac{D\boldsymbol{U}}{Dt} + \mu \nabla^2 \boldsymbol{U}, \qquad (1)$$

where P represents the instantaneous pressure, $\boldsymbol{U}$ is the velocity vector, ρ density and μ is the dynamic viscosity. At the right-hand side the symbol $\frac{D}{Dt}$ indicates the material derivative of the velocity field that requires a 3D time-resolved measurement. The pressure field can be calculated by a direct spatial integration scheme starting from a given value or line distribution as boundary conditions (Baur and Köngeter 1999; Liu and Katz 2006). However, the present work follows the approach proposed by Gurka et al. (1999) and de Kat et al. (2010) whereby the problem is formulated in terms of the Poisson pressure equation. The latter is obtained by applying the divergence operator to equation (1) resulting in:

$$\nabla^2 P = -\rho \nabla . \frac{D\boldsymbol{U}}{Dt} + \mu \nabla . [\nabla^2 \boldsymbol{U}]. \qquad (2)$$

The terms on the right-hand side are measured by time-resolved tomographic PIV, yielding simultaneously the velocity vector, the velocity gradient tensor and the temporal derivative of the velocity. The derivatives are evaluated by central finite differences both in space and time. Once the right-hand side term is evaluated, the Poisson problem is solved applying boundary conditions of Dirichlet type on the outer edge of the boundary layer (constant and uniform pressure) and of Neumann type elsewhere. A detailed discussion of the data reduction procedure and of the measurement uncertainties, is given by de Kat and van Oudheusden (2011).

3 Experimental apparatus

The experiments were performed in an open test-section vertical wind tunnel located at the Aerodynamics Laboratories of Delft University of Technology. The circular cross-section has a diameter of 0.6 m. The flow velocity at the exit is 10 m/s and the turbulence intensity in the free stream is about 0.02%. A flat plate 2 m long with an elliptical leading-edge and a sharp symmetric trailing-edge as shown in Figure 1 is used to form the turbulent boundary layer. The plate spans the entire test section and is installed at zero angle-of-attack. Laminar-to-turbulent transition of the boundary layer is forced at 150 mm downstream of the leading edge.

Pressure fluctuations at the wall are measured using two electret condenser Sonion 8010T microphones. The two microphones are placed at 10 mm distance along the x-direction. They can measure fluctuations from 10 to 20,000 Hz with a flat frequency response from 250 Hz to 7,500 Hz.

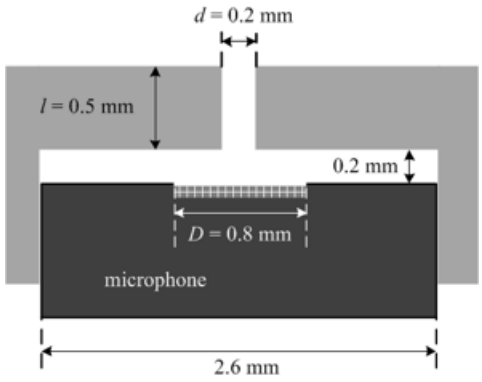

Figure 1: Schematic drawing of the microphone installation under the plate surface.

The microphone has a sensitivity of -33.5 dB at 1 kHz, equivalent to 21 mV/Pa. The typical sound pressure level of the equivalent noise is 26.5 dB (A-weighted). These electret microphones provide a similar sensitivity in comparison to the typical ½ or ¼ inch condenser microphones while their smaller physical dimension of 2.56 mm in diameter (microphone orifice size of D = 0.8 mm) makes them suitable for measurement of small scale fluctuations. The analog signal is conditioned by a low-pass filter starting at 10.6 kHz followed by an amplifier. The signals are sampled at 50 kHz using a National Instrument NI-9215 data acquisition system with 16 bits resolution. The data acquisition is synchronized with the PIV acquisition system. The sequence recording is triggered by an external signal (output from the PIV system) to a high-speed digital I/O NI-9401 module placed in a NI cDAQ-9172 chassis also holding the NI-9215.

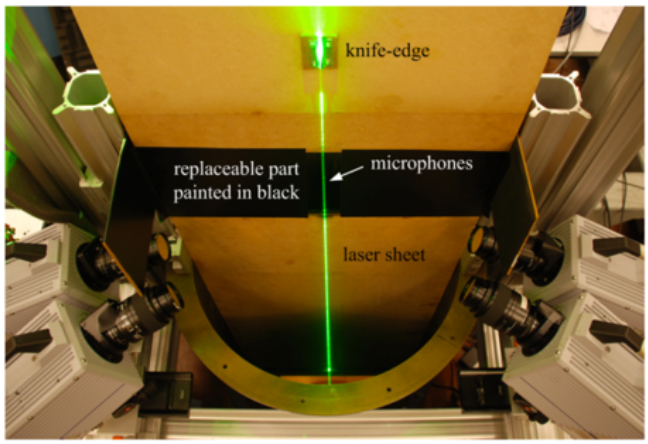

Figure 2: Experimental setup of Tomo-PIV system to measure the turbulent boundary layer on flat plate.

4 Results

The detailed velocity profile of the boundary layer is obtained from planar PIV measurements (2C-PIV) that also serve as a basis to evaluate the accuracy of the Tomo-PIV velocity measurement. The 2C-PIV velocity vectors are obtained from the average of the correlation maps allowing a spatial resolution of 21 vectors/mm equivalent to a vector pitch of $1.2\lambda^+$ (including 75 % overlap). This high spatial resolution enables measurement within the inner layer and provides access to the inner layer variables (u_τ and λ^+) that are used to scale the Tomo-PIV velocity profiles. The boundary layer profile of this figure follows the law of the wall ($u^+ = y^+$) and the log law ($u^+ = \frac{1}{0.4}\ln(y^+) + 5.5$) as shown with the dash line. The inner layer (viscous sublayer and the buffer layer) covers about 1 mm from the wall while the overlap layer (logarithmic layer) is at $y = 1$ till 8 mm. The edge of the boundary layer is measured at 30 mm from the wall.

The turbulent fluctuations are measured using both 2C-PIV (detailed in the second column of Table 2) and Tomo-PIV (detailed in the first column of Table 3). The results show the typical trend of $\langle u^2 \rangle$, $\langle v^2 \rangle$ and $\langle uv \rangle$ within a zero pressure gradient turbulent boundary layer (Klebanoff, 1954) and a rather good agreement is observed between the two measurement systems, with a slight discrepancy at the outer layer due to the different free stream velocities.

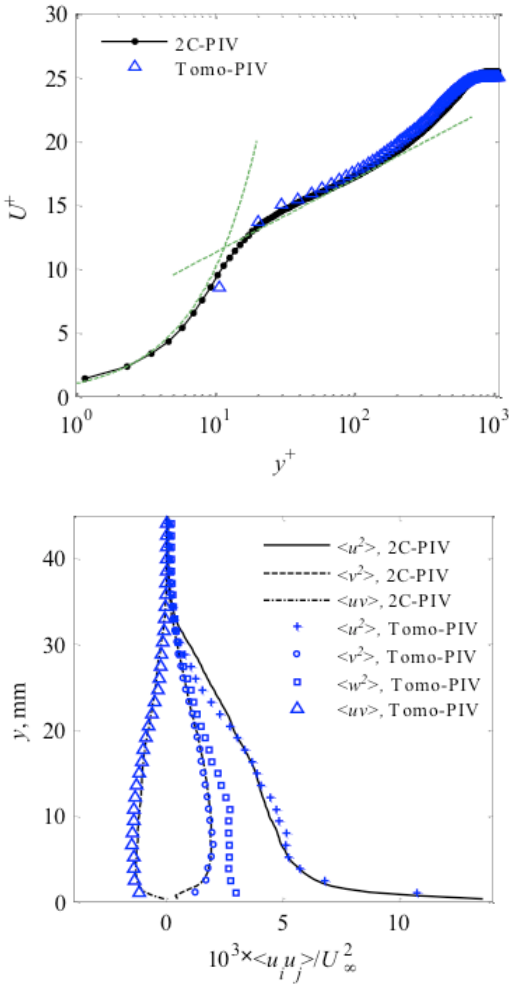

Figure 3: (top) turbulent boundary layer profile in semi-log scale measured by 2C-PIV and Tomo-PIV. (bottom) Normal and Reynolds shear stresses.

The power spectral density (PSD) of the surface pressure fluctuations and the PSD of the velocity magnitude at $y = 2$ mm above the wall are shown in Figure 4. The PSD is calculated with a frequency resolution f_{res}=100 Hz using Hanning window with effective noise bandwidth (ENBW) of 151.5 Hz. The PSD of the pressure fluctuations is shown in the range of 250 to 7,500 Hz where the microphones have a constant sensitivity. Although a reduction of the energy with increase of frequency is observed, a wide range of pressure fluctuations are required to be captured for proper flow characterization. For example, if two orders of magnitude energy band is of interest, pressure fluctuations up to 4 kHz should be captured requiring a PIV repetition rate of at least 8 kHz according to the Nyquist criterion.

The PSD of the streamwise velocity fluctuations (u) is also calculated from the time-resolved 2C-PIV and Tomo-PIV data which are acquired at 10 kHz. The different data series refer to the cross-correlation analysis from a single pair of images or multiple pairs. When 3 pairs are considered the measurement time corresponds to 300 μs. The PSDs obtained from 2C-PIV and Tomo-PIV with a single pair show similar energy distribution varying over approximately three decades up to a frequency of approximately 3 kHz, where the distribution reaches a plateau ascribed to measurement noise. The use of two and three pairs decreases the noise level by about one order of magnitude. However, this also results in an earlier drop of the spectral energy at lower frequency, which may indicate a reduction of the temporal resolution. Any further increase of the correlation-averaging kernel (number of pairs) will reduce significantly the temporal resolution and the case of more than 3 pairs is not considered in the present work.

The discrepancy between the 2C-PIV and Tomo-PIV is also observed to increase by using a higher number of correlation pairs. The lowest noise background corresponds to 3 pairs correlation of Tomo-PIV data which is about 10^{-7} $(m/s)^2/Hz$. This is equivalent to the measurement noise of 0.02 m/s obtained by integrating the background noise over the PSD frequency range (0-5 kHz).

The pressure field obtained from the time-resolved Tomo-PIV system provides an indirect volumetric measurement of pressure within the turbulent boundary layer. To the authors knowledge this is the first experiment where the flow field pressure is measured in a turbulent boundary layer, since previous measurements where conducted using point-wise measurement techniques. The pressure field in a turbulent boundary layer consists of minute pressure fluctuations: in the present experiment, the typical amplitude is in the order of 1 Pa as shown in the instantaneous pressure fields shown in the remainder.

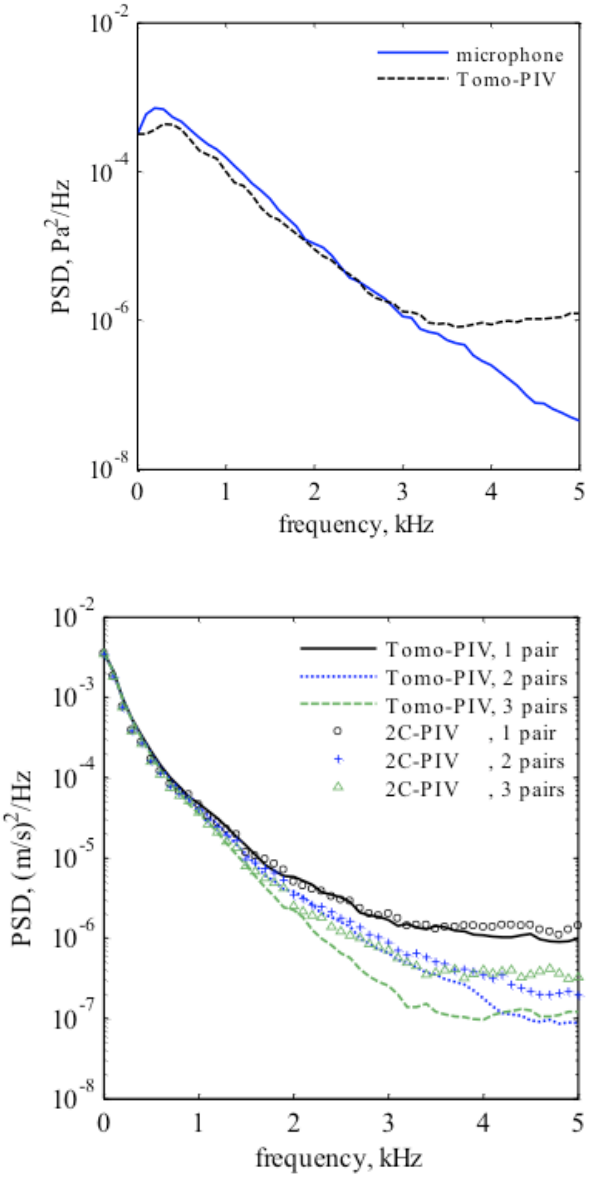

Figure 4: (top) PSD of the surface pressure fluctuations. (bottom) PSD of the velocity magnitude measured using Tomo-PIV. Results obtained from correlation of 1, 2 and 3 image pairs.

The pressure field obtained from the measurements after solving eq. 2, shows small blobs of relatively strong fluctuations adjacent to the wall while larger blobs of much weaker amplitude travel further away from the wall (Figure 5). It is also observed that the highest pressure fluctuation (adjacent blobs of low and high pressure) exist till about 7 mm distance from the wall (the inner and the overlap layers). Further away from the wall, the outer layer fluctuations become even smaller, with amplitude of about 0.2 Pa. Vortex identification using three-dimensional formulation of the Q criterion (Hunt *et al.* 1988) shows the overlap of the vortex cores and the regions of minimum local pressure. Three vortex cores identified as A, B, and C belong to the heads of three hairpin vortices traveling together within a hairpin packet (Adrian *et al.* 2000). In the magnified view (Figure 5-bottom) it is clearly observed that the vortex heads coincide with low-pressure regions. The positive pressure blob in between the vortex cores A and B is due to the stagnation region caused by the opposite inductions of the sweep event of vortex A and the ejection event of vortex B. This high-pressure region is along the shear layer between the two hairpin vortices (Johansson et al., 1987).

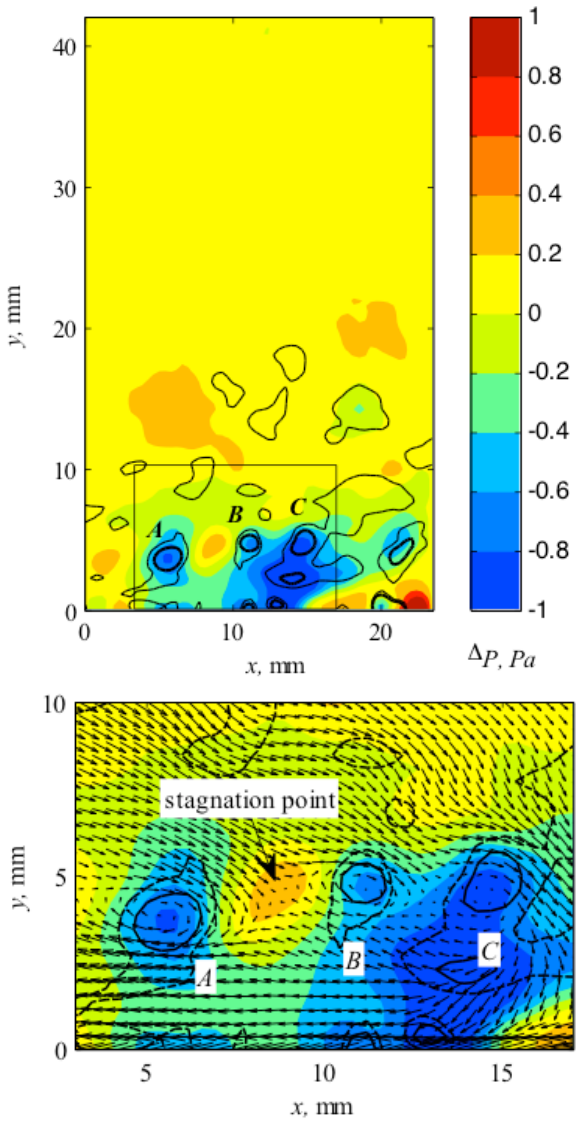

Figure 5: (top) Snapshot of pressure fluctuations along with two contours of Q-criterion (solid thin and thick lines) obtained from Tomo-PIV. The pressure difference is relative to a reference pressure outside the boundary layer. (bottom) Magnified view of the rectangular box containing the vortex heads A, B, and C. The velocity vectors are shown in a convective frame of reference at $U = 0.78U_\infty$.

5 Uncertainty analysis

Such novel measurements require a thorough scrutiny of the attainable precision for the instantaneous pressure. The verification is made by comparison of the pressure obtained by PIV and that measured by the wall-mounted transducer.

The fluctuating pressure signal obtained from the Tomo-PIV system and the simultaneous surface pressure measurement using the electret microphone are shown over a 20 ms time span in Figure 6. Both the signals are band-pass filtered between 250 to 3500 Hz in which the lower limit of 250 Hz is applied due to the non-linear sensitivity of the microphone. The upper limit takes into account the sampling frequency of the PIV system and the 3-pairs analysis. A close agreement of the Tomo-PIV pressure and the microphone surface pressure measurement is observed

in the time diagram. The comparison is further quantified by temporal cross-correlation (R_{pp}) between the two pressure signals measured simultaneously by the Tomo-PIV and the surface microphone at the same wall location (pinhole location). The rms of pressure measured by the PIV and the microphones are σ_{PIV} = 0.49 and σ_{mic} = 0.57 band-pass filtered between 250-3500 Hz. A cross-correlation coefficient of R_{pp}=0.6 is obtained in the present experiments.

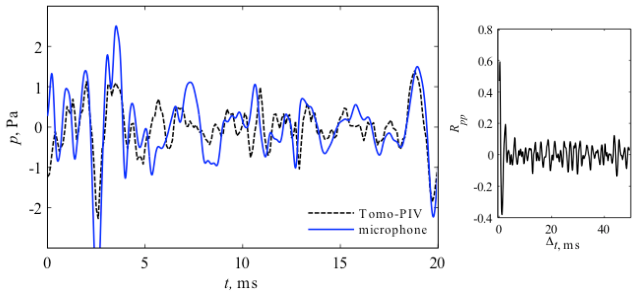

Figure 6: Comparison of the pressure signal measured by the surface microphone and from Tomo-PIV in time-domain and by cross-correlation coefficient.

The pressure signal shows high amplitude peaks of negative or positive pressure at t = 2.5, 3.5. 19 and 19.7 ms.

Similar high amplitude peaks have also been previously observed in the wall pressure signals by Schewe (1983) and further investigated by Johansson et al. (1987) and Kim (1989). Different threshold levels were considered to detect these structures, however, the peaks are typically reported to be about $3\times p_{rms}$ and have a duration of about 10-15t^* ($t^* = \nu / u_\tau^2$) according to Johansson et al. (1987) that is equivalent to 1.7 Pa and 1.1-1.5 ms in the current experiment. It is observed that the negative pressure peaks are caused by a vortex core passing over the surface at x = 15 mm. Instead, positive pressure fluctuations as that observed at t = 19 ms is ascribed to local flow stagnation between ejection and sweep regions, corresponding to saddle points.

The space-time diagram is used to visualize the pressure fluctuations as they evolve along the measured spatial interval. An alternating arrangement of positive and negative fluctuations is observed with an inclination that corresponds to a convection velocity of about 5.6 m/s (0.6U_c). This shows the dominant contribution of the inner layer structures to the wall pressure fluctuations. The coherence time for such events is captured by the present measurement as most events are observed to begin and end within the measurement interval. Both positive and negative fluctuations remain coherent for approximately 1 to 2 ms, consistent with the time-scale of the high-amplitude peaks (Johansson et al. 1987). The latter estimate will be in defect when the structures causing such pressure fluctuations travel also in the transverse direction. It also appears that positive fluctuations of high amplitude are strongly correlated with preceding negative fluctuations. This is associated to the passage of a packet of vortices close to the wall. Further scrutiny of the spatio-temporal organization of the pressure fluctuations goes beyond the scope of the present study.

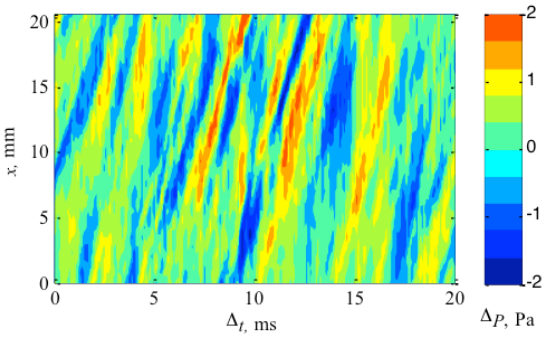

Figure 10: Space-time diagram of surface pressure fluctuations.

6 Conclusion

The surface pressure fluctuations caused by boundary layer turbulence have been measured by a technique based on time-resolved Tomo-PIV. The measurements were conducted at 10 kHz and the results were compared to the surface pressure signal measured at a point using an electret condenser microphone. The comparison shows agreement with cross-correlation coefficient of 0.6 and a good agreement of the spectral properties up to 3 kHz.

The study demonstrates that PIV can be adopted as non-intrusive diagnostic tool to assess simultaneously the velocity/vorticity distribution in the flow field and the associated pressure field.

Current efforts are directed at obtaining the pressure distribution over an extended region of the surface, which will enable to use it as input for the evaluation of acoustic source following Curle's analogy.

Acknowledgments

This research is supported by the European Research Council (ERC) under the the FLOVIST project (Flow Visualization Inspired Aeroacoustics with Time Resolved Tomographic Particle Image Velocimetry). Grant no 202887.

References

[1] T. Baur, J. Köngeter, "PIV with high temporal resolution for the determination of local pressure reductions from coherent turbulent phenomena" *3rd International Workshop on Particle Image Velocimetry*, Santa Barbara (US), (1999)

[2] W.K. Blake, "Turbulent boundary-layer wall-pressure fluctuations on smooth and rough walls", *J. Fluid Mech.*, 44, 637-660 (1970)

[3] P.A. Chang, U. Piomelli, W.K. Blake, "Relationship between wall pressure and velocity-field sources", *Phys. Fluids*. 11, 3434-3448 (1999)

[4] R. de Kat, B.W. van Oudheusden "Instantaneous planar pressure determination from PIV in turbulent flow", *Exp. Fluids*. (2011)

[5] J.E. Ffowcs Williams, L.H. Hall, "Aerodynamic sound generation by turbulent flow in the vicinity of a

scattering half plane", *J. Fluid Mech.* 40, 657-670 (1970)

[6] J.C.R. Hunt, A.A. Wray, P. Moin "Eddies, stream, and convergence zones in turbulent flows", *Research Report CTR-S88*, 193-208. Center for Turbulence (1988)

[7] A.V. Johansson, P.H. Alfredsson, J. Kim, "Evolution and dynamics of shear-layer structures in near-wall turbulence", *J. Fluid Mech.* 224, 579-599 (1991)

[8] J. Kim, J. Choi, H.J. Sung "Relationship between wall pressure fluctuations and streamwise vortices in a turbulent boundary layer", *Phys. Fluids* 14, 898-901 (2002)

[9] X. Liu, J. Katz "Instantaneous pressure and material acceleration measurements using a four-exposure PIV system", *Exp. Fluids* 41, 227-240 (2006)

[10] G. Schewe "On the structure and resolution of wall-pressure fluctuations associated with turbulent boundary-layer flow", *J. Fluid Mech*. 134, 311-328 (1983)

[11] Y. Tsuji, J.H.M. Fransson, P.H. Alfredsson, A.V. Johansson, "Pressure statistics and their scaling in high-Reynolds-number turbulent boundary layers", *J. Fluid Mech.* 585, 1-40 (2007)

[12] Willmarth, W.W. 1956 Wall pressure fluctuations in a turbulent boundary layer. J. Acoust. Soc. Am. 28:1048.

[13] Willmarth, W.W. 1975 Pressure fluctuations beneath turbulent boundary layers. Ann. Rev. Fluid Mech 7:13-36